

Nanowire formation on sputter eroded surfaces

J. Kim,¹ B. Kahng,¹ and A.-L. Barabási²

¹ School of Physics and Center for Theoretical Physics,
Seoul National University, Seoul 151-747, Korea

² Department of Physics, University of Notre Dame, Notre Dame, IN 46556

Rotated ripple structures (RRS) on sputter eroded surfaces are potential candidates for nanoscale wire fabrication. We show that the necessary condition for RRS formation is that the width of the collision cascade in the longitudinal direction has to be larger than that in the transverse direction, which can be achieved by using high energy ion beams. By calculating the structure factor for the RRS we find that they are more regular and their amplitude is more enhanced compared to the much studied ripple structure forming in the linear regime of sputter erosion.

The fabrication of nanoscale surface structures such as quantum dots (QDs) and quantum wires (QWs), have attracted considerable attention due to their applications in optical and electronic devices [1]. These nanostructures form thanks to various self-assembled mechanisms, induced by the combined effect of strain and growth kinetics. Yet, the strained nanostructures obtained by these methods have a size distribution wider than required by applications, and display random alignment. Lithographic methods [2] are often considered prime candidates to overcome these shortcomings, but their limited resolution offers further challenges. Consequently, there is continued high demand for alternative methods that would allow low cost and efficient mass fabrication of nanoscale surface structures. In the light of these technological and scientific driving forces, the recent demonstration by Facsko *et al.* that low-energy (40 eV \sim 1.8 keV) normal incident Ar⁺ sputtering on GaSb (100) surfaces leads to nanoscale islands which display remarkably good hexagonal ordering and have a uniform size distribution, has captured the interest of the scientific community [3,4].

It is known that the morphological evolution of a sputter eroded surface is well approximated by the noisy nonlinear Kuramoto-Sivashinsky (KS) equation,

$$\partial_t h = \nu_x \partial_x^2 h + \nu_y \partial_y^2 h - D_{xx} \partial_x^4 h - D_{yy} \partial_y^4 h - D_{xy} \partial_x^2 \partial_y^2 h + \frac{\lambda_x}{2} (\partial_x h)^2 + \frac{\lambda_y}{2} (\partial_y h)^2 + \xi(x, y, t), \quad (1)$$

where ν_x and ν_y are the effective surface tensions generated by the erosion process; D_{xx} , D_{yy} , and D_{xy} are the ion induced effective diffusion constants; λ_x and λ_y describe the tilt-dependent erosion rates in each direction; and $\xi(x, y, t)$ is an uncorrelated white noise with zero mean, mimicking the randomness resulting from the stochastic nature of ion arrival to the surface [5,6]. At low temperatures all the coefficients in Eq. (1) depend on experimental parameters such as the ion beam flux f , the ion beam energy ϵ , and the incidence angle of ion beam θ [7], while at high temperatures D depends on surface temperature. For the sputter erosion process $\nu < 0$ and $D > 0$, while the signs of λ_x and λ_y vary depending on the incident angle of the ion beam.

Recently numerical simulations have shown that there

is a clear separation of the linear and nonlinear regimes in time [8]: Up to a crossover time τ_1 the surface is eroded as if the nonlinear terms would be completely absent, following the predictions of the linear theory [9] (i.e. $\lambda_x = \lambda_y = 0$ in Eq. (1)). After τ_1 , however, the nonlinear terms with coefficients λ_x and λ_y take over and completely determine the surface morphology. The transition from the linear to the nonlinear regime can be seen either by monitoring the surface width (which is proportional to the ripple amplitude) or the erosion velocity.

In the nonlinear regime the case $\lambda_x \lambda_y < 0$ is in particular interesting. The surface morphology in this case exhibits another transition from kinetic roughening to a rotated ripple structures (RRS) at a second crossover time τ_2 ($\tau_2 > \tau_1$), as first predicted by Rost and Krug [10], and observed numerically in [8]. Moreover, it was found that the RRS is straighter than the ripple pattern forming in the linear regime, making it a potential candidate for nanowire fabrication. In this Letter we investigate the necessary conditions for the formation of RRSs and the impact of the various experimentally controllable parameters on the morphology of the RRS. We find that at low temperatures the RRSs form when the longitudinal width (σ) of the damage cascade generated by the ion beam is larger than the transverse width (μ), which can be achieved for high energy (ϵ). When the energy is too high, however, the crossover time τ_2 becomes too long. Thus, we predict that the RRS structure could be obtained in a moderate range of the incident energy, using an appropriate exposure time and low temperatures.

Rotated ripple structures form when $\lambda_x \lambda_y < 0$ and the rotation angle is given by $\phi_c = \tan^{-1} \sqrt{-\lambda_x / \lambda_y}$. As shown in Fig. 1, the angle ϕ_c increases with the ratio $a_\mu = a / \mu$, but decreases with the incident angle θ , where a denotes the penetration depth of the ion beam and a_μ depends on the ion beam energy ϵ . The KS equation in the rotated frame can be written in the same form as Eq. (1) except that the coefficients ν , D , and λ are replaced by ν' , D' , and λ' , which are functions of those in the original frame and the angle ϕ_c . In the rotated frame one of the coefficients of the nonlinear terms, say $\lambda'_{x'}$, is equal to zero, and the other is given by $\lambda'_{y'} = \lambda_x + \lambda_y$, where (x', y') represents the coordinates in the rotated frame. Since $\lambda'_{x'}$ vanishes, the dynamic equation in the

x' direction becomes linear. Consequently, the ripple pattern is along the x' direction as long as (i) $\nu'_{x'} < 0$; (ii) $D'_{x'x'} > 0$; and (iii) $\lambda_x \lambda_y < 0$. Therefore the conditions (i), (ii), and (iii) are the necessary conditions for the formation of the RRS.

We investigate the satisfiability of these conditions in the parameter space $(\theta, a_\mu = a/\mu)$ for different values of $a_\sigma = a/\sigma$. We find that when $a_\mu > 1$ and $a_\sigma = 1$ or $a_\mu > 2$ and $a_\sigma = 2$, the RRS can form in the region depicted in Fig. 2. For $a_\mu < 1$ given $a_\sigma = 1$, the shaded region satisfying (i) – (iii) scarcely exists, so that the formation of RRS is less likely. That means the RRSs are expected to form when the longitudinal width σ is larger than the transverse width μ , that is, $\sigma > \mu$. Recent experimental results indicate that for graphite surfaces σ depends on ϵ , while μ is independent of ϵ for large ϵ ($2 \sim 50$ keV) [11]. Therefore, the $\sigma > \mu$ condition can be met when the energy of the incident ion beam is high enough. Thus in order to obtain the RRS experimentally it is desirable to use high energy ion beam with an appropriate choice of the incident angle (Fig. 2). However, the use of a high energy ion beam increases τ_2 rapidly, requiring a longer exposure time.

Since the nonlinear term disappears in the x' direction the surface in this direction is driven by a linear instability. The amplitude of the RRS grows exponentially with time until the nonlinear term in the y' direction becomes effective, after which the amplitude saturates. Meanwhile, the surface in the y' direction displays kinetic roughening due to the presence of the nonlinear term $\lambda'_{y'}(\partial_{y'}h)^2/2$, so that the roughness in the y' direction is considerably reduced compared with the roughness in the x' direction. Therefore the RRS develops a rough morphology in the x' direction, while it is relatively smooth in the y' direction, the end configuration resembling a V-shaped wire pattern, as shown in Fig. 3 [12]. The RRS formed in the nonlinear regime is comparable with the ripple pattern formed in the linear regime, where there are modulations in both directions, and the roughness in each direction is almost of the same order.

We also examined the structure factor

$$S(\mathbf{q}) = \int \frac{d\mathbf{r}}{(2\pi)^2} \exp(i\mathbf{q} \cdot \mathbf{r}) H(\mathbf{r}), \quad (2)$$

where $H(\mathbf{r})$ is the height-height correlation function,

$$H(\mathbf{r}, t) = \left\langle \sum_{\mathbf{r}'} h(\mathbf{r}' + \mathbf{r}, t) h(\mathbf{r}', t) \right\rangle - \left\langle \sum_{\mathbf{r}'} h^2(\mathbf{r}', t) \right\rangle, \quad (3)$$

averaged over different configurations [13]. We find that the structure factor exhibits a peak at $(q_{x,c}, q_{y,c})$, corresponding to $(q'_{x',c}, 0)$ in the rotated coordinates (Fig. 4). The fact that $q'_{y',c} = 0$ confirms that the RRS is straight in the y' direction. Moreover, the amplitude of the structure factor for the RRS is much larger compared to the

ripple formed in the linear regime, as shown in the inset of Fig. 4. Accordingly, the RRS could be a good candidate for the fabrication of nanowires.

Applying the linear instability theory in the x' direction we obtain the wavelength of the RRSs $\ell'_{x'} = 2\pi\sqrt{2D'_{x'x'}/|\nu'_{x'}|}$. The wavelength depends on the penetration depth linearly, i.e. $\ell'_{x'} \sim a$, independent of the ion flux f . In general, the penetration depth depends on the incident ion energy ϵ as $a \sim \epsilon^{2m}$, where $m \approx 1/4$ was obtained recently for the nanoscale dot structure in low energy sputtering [14]. We also examined $\ell'_{x'}$ in function of the ratio a_μ and incident angle θ , observing a monotonically increasing and decreasing behavior, respectively (Fig. 5).

In the high temperature limit the wavelength of the RRS depends on the ion energy as $\ell'_{x'} \sim \epsilon^{-1/2}$, and on the ion flux as $\sim f^{-1/2}$, and on the temperature as $\sim \exp(-\epsilon/4kT)$, a dependence similar to that observed during the formation of nanoscale dots [15].

In summary, we examined the necessary conditions for the formation of RRSs, potential candidates for nanowires for electron transport. We predict that the RRS can be generated under high energy ion beam, in contrast with the formation of nanoscale dots structure occurring during low energy ion beam sputtering. Since high energy ion beam causes longer crossover time for the formation of the RRS, exposure time of the ion beam has to be adjusted to obtain the desired RRS.

This work was supported by ONR, the Korean Research Foundation (Grant No. 99-041-D00150), NSF-DMR 01-08494 and NSF-INT 99-10426.

-
- [1] For a review, for example, see L. Jacak, P. Hawrylak, and A. Wojs, *Quantum dots* (Springer-Verlag, Berlin, 1998).
 - [2] T.I. Kamins and R.S. Williams, Appl. Phys. Lett. **71**, 1201 (1997).
 - [3] S. Facsko, T. Dekorsy, C. Koerdts, C. Trappe, H. Kurz, A. Vogt, and H.L. Hartnagel, Science **285**, 1551 (1999).
 - [4] F. Frost, A. Schindler, and F. Bigl, Phys. Rev. Lett. **85**, 4116 (2000).
 - [5] R. Cuerno and A.-L. Barabási, Phys. Rev. Lett. **74**, 4746 (1995).
 - [6] M.A. Makeev and A.-L. Barabási, Appl. Phys. Lett. **71**, 2800 (1997).
 - [7] M. Makeev, R. Cuerno, and A.-L. Barabási (preprint).
 - [8] S. Park, B. Kahng, H. Jeong, and A.-L. Barabási, Phys. Rev. Lett. **83**, 3486 (1999).
 - [9] R.M. Bradley and J.M.E. Harper, J. Vac. Sci. Technol. A **6**, 2390 (1988).
 - [10] Rost and J. Krug, Phys. Rev. Lett. **75**, 3894 (1995).
 - [11] S. Habenicht, W. Bolse, H. Feldermann, U. Geyer, H. Hofsaß, K.P. Lieb, F. Roccaforte, Europhys. Lett. **50**, 209 (2000).

- [12] E. Kapon, D. Hwang, and R. Bhat, Phys. Rev. Lett. **63**, 430 (1989).
- [13] S.K. Sinha, E.B. Sirota, S. Garoff, and H.B. Stanley, Phys. Rev. B **38**, 2297 (1988).
- [14] S. Facsco, H. Kurz, and T. Dekorsy, Phys. Rev. B **63**, 165329 (2001).
- [15] B. Kahng, H. Jeong, and A.-L. Barabási, Appl. Phys. Lett. **78**, 805 (2001).

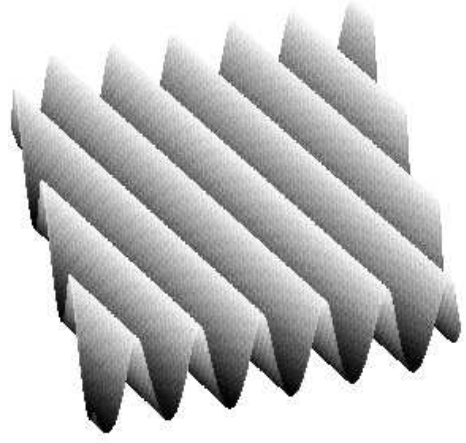


FIG. 3. Surface morphology of the RRS, as generated by numerical simulations, with $a_\mu = 1.3$, $a_\sigma = 1$ and $\theta = 43.56$ degree.

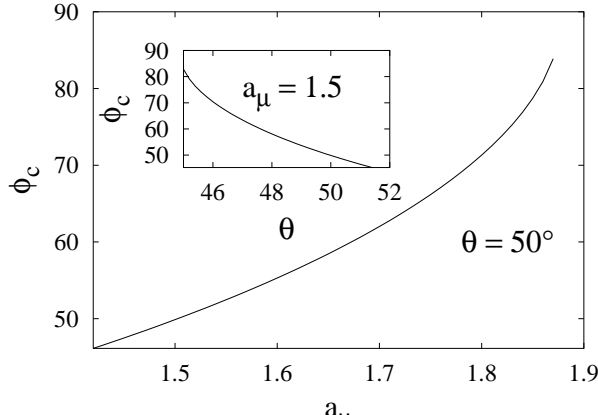


FIG. 1. The rotation angle ϕ_c as a function of a_μ at $\theta = 50$ degree. The inset shows ϕ_c versus θ for $a_\mu = 1.5$. The rotation angle increases as the ratio a_μ increases, but decreases with the incident angle θ .

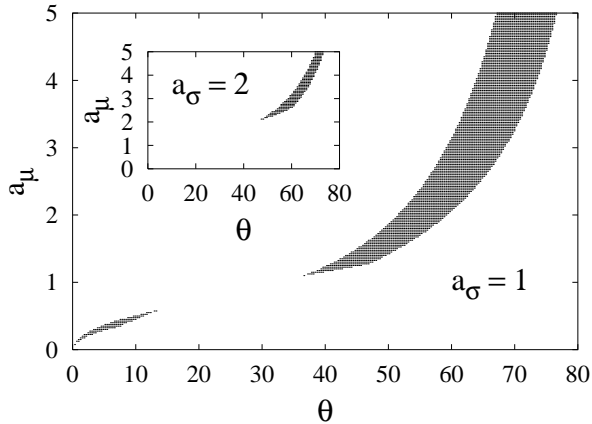


FIG. 2. The shaded region in the parameter space (θ, a_μ) for $a_\sigma = 1$ (inset: for $a_\sigma = 2$) corresponds to the region where the RRS can form.

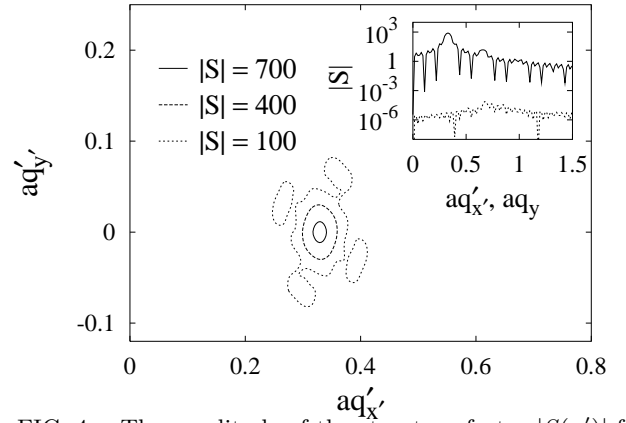


FIG. 4. The amplitude of the structure factor $|S(\mathbf{q}')|$ for the RRS shown in Fig. 3. The peak of the structure factor is at $aq'_{x,c} = 0.33$ and $aq'_{y,c} = 0$, implying that the wire structure is straight along the y' axis. The inset shows the comparison between the amplitudes of the structure factor for the RRS (solid line) and for the linear ripple (dotted line), implying the amplitude of the RRS is about a factor of 10^7 larger compared to that of the ripple structure formed in the linear regime.

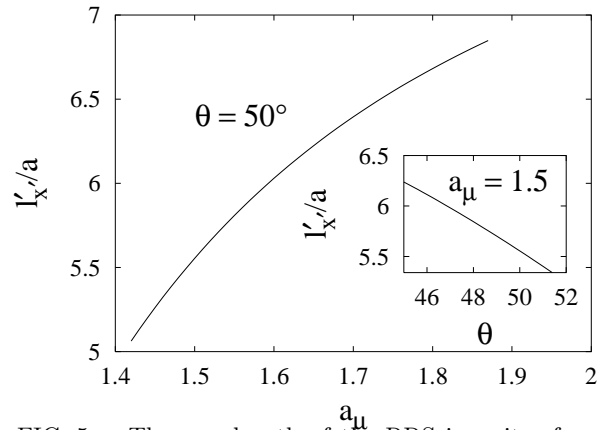


FIG. 5. The wavelength of the RRS in units of a as a function of a_μ ($\theta = 50$ degree). Inset: The wavelength versus θ at $a_\mu = 1.5$.